Article

Cell Host & Microbe

Recent H3N2 Viruses Have Evolved Specificity for Extended, Branched Human-type Receptors, Conferring Potential for Increased Avidity

Graphical Abstract

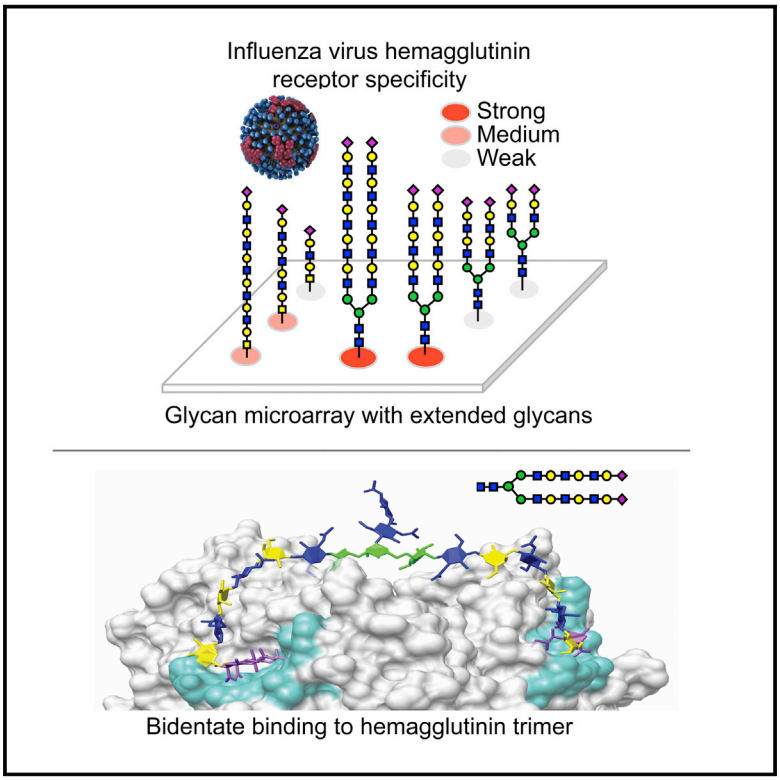

Authors

Wenjie Peng, Robert P. de Vries, Oliver C. Grant, ..., Ian A. Wilson, Robert J. Woods, James C. Paulson

Correspondence

jpaulson@scripps.edu

In Brief

To clarify H3N2 human influenza virus receptor specificity, Peng et al. developed a glycan array that included extended glycans. Recent H3N2 and 2009 pandemic H1N1 viruses share specificity for human-type receptors with extended glycan chains, conferring potential for increased avidity by simultaneously binding two subunits of a single hemagglutinin trimer.

Highlights

- All H3N2 influenza viruses recognize human-type receptors with extended glycan chains
- Recent H3 and pandemic H1 hemagglutinins prefer extended, branched N-glycan receptors
- Lipid-linked glycan receptors restore infectivity to receptor-deficient MDCK cells
- Molecular dynamics simulation shows bidentate binding of N-glycans to one HA trimer

Peng et al., 2017, Cell Host & Microbe *21*, 23–34
January 11, 2017
http://dx.doi.org/10.1016/j.chom.2016.11.004

Cell Host & Microbe
Article

Recent H3N2 Viruses Have Evolved Specificity for Extended, Branched Human-type Receptors, Conferring Potential for Increased Avidity

Wenjie Peng,[1,5] Robert P. de Vries,[1,5,6] Oliver C. Grant,[2] Andrew J. Thompson,[1] Ryan McBride,[1] Buyankhishig Tsogtbaatar,[1] Peter S. Lee,[3,7] Nahid Razi,[1] Ian A. Wilson,[3,4] Robert J. Woods,[2] and James C. Paulson[1,8,*]
[1]Departments of Cell and Molecular Biology, Chemical Physiology, and Immunology and Microbial Science, The Scripps Research Institute, La Jolla, CA 92037, USA
[2]Complex Carbohydrate Research Center, University of Georgia, Athens, GA 30602, USA
[3]Department of Integrative Structural and Computational Biology, The Scripps Research Institute, La Jolla, CA 92037, USA
[4]Skaggs Institute for Chemical Biology, The Scripps Research Institute, La Jolla, CA 92037, USA
[5]Co-first author
[6]Present address: Department of Chemical Biology and Drug Discovery, Utrecht Institute for Pharmaceutical Science, Utrecht University, Utrecht 3584, the Netherlands
[7]Present address: Department of Pharmaceutical Chemistry, University of California, San Francisco, Mission Bay, San Francisco, CA 94158, USA
[8]Lead Contact
*Correspondence: jpaulson@scripps.edu
http://dx.doi.org/10.1016/j.chom.2016.11.004

SUMMARY

Human and avian influenza viruses recognize different sialic acid-containing receptors, referred to as human-type (NeuAcα2-6Gal) and avian-type (NeuAcα2-3Gal), respectively. This presents a species barrier for aerosol droplet transmission of avian viruses in humans and ferrets. Recent reports have suggested that current human H3N2 viruses no longer have strict specificity toward human-type receptors. Using an influenza receptor glycan microarray with extended airway glycans, we find that H3N2 viruses have in fact maintained human-type specificity, but they have evolved preference for a subset of receptors comprising branched glycans with extended poly-N-acetyl-lactosamine (poly-LacNAc) chains, a specificity shared with the 2009 pandemic H1N1 (Cal/04) hemagglutinin. Lipid-linked versions of extended sialoside receptors can restore susceptibility of sialidase-treated MDCK cells to infection by both recent (A/Victoria/361/11) and historical (A/Hong Kong/8/1968) H3N2 viruses. Remarkably, these human-type receptors with elongated branches have the potential to increase avidity by simultaneously binding to two subunits of a single hemagglutinin trimer.

INTRODUCTION

Human and animal influenza viruses are classified by the antigenic serotypes of the two major surface glycoproteins, hemagglutinin (HA), which binds to sialic acid containing receptors on the host cell, and neuraminidase (NA), which destroys receptors and releases virus progeny from infected cells. Although 18 HA and 11 NA serotypes are found in influenza A viruses that circulate in avian and mammalian species, only three combinations have successfully adapted to humans (H1N1, H2N2, and H3N2) (Yoon et al., 2014). Currently, only two viral subtypes circulate within humans: H3N2, which emerged in the population in 1968, and the novel H1N1 (pandemic H1N1) established in 2009, which replaced the seasonal H1N1 strains.

Human viruses and their avian virus progenitors differ in their receptor specificity, which is believed to represent a major barrier for avian virus transmission in humans (de Graaf and Fouchier, 2014; Imai and Kawaoka, 2012; Paulson and de Vries, 2013; Raman et al., 2014; Shi et al., 2014). Human influenza viruses prefer receptors that are sialic acid α2-6 linked to galactose (human-type), which are dominant on epithelial cells of the human airway. In contrast, avian influenza viruses exhibit preferred recognition of receptors with sialic acid α2-3 linked to galactose (avian-type) and bind poorly to human airway epithelium. In previous human pandemics (H1, H2, and H3) that originated from avian viruses, only two amino acid mutations in the receptor-binding pocket of the HA were sufficient to produce a switch from avian-type to human-type specificity, providing a molecular basis for this simple receptor paradigm (Connor et al., 1994; Matrosovich et al., 2000; Skehel and Wiley, 2000; Stevens et al., 2006).

Evolution of H3N2 influenza viruses through antigenic drift has produced changes in receptor binding that have begun to blur the definition of human-type receptor specificity (Li et al., 2013; Lin et al., 2012). Changes in receptor-binding properties were first noticed by the lack of agglutination of red blood cells in hemagglutination assays and the difficulty in recovery of virus from patient samples through propagation in laboratory hosts (e.g., eggs and MDCK cells). Moreover, recent H3 isolates showed increasingly reduced avidity and inconsistent specificity for

human-type receptors in receptor-binding assays (Gulati et al., 2013; Lin et al., 2012; Medeiros et al., 2001; Nobusawa et al., 2000; Stevens et al., 2010; Yang et al., 2015). These observations have suggested that human H3N2 viruses have not maintained consistent receptor specificity during evolution in the human population.

While the terms human-type and avian-type receptor specificity refer to the sequences NeuAcα2-6Gal versus NeuAcα2-3Gal, respectively, these are the terminal sequence fragments found on a diverse array of glycans that decorate glycoproteins on the surface of a cell. Thus, these terms belie the true complexity of the glycome and the potential for other aspects of glycan structure to be important factors in receptor recognition. Glycan profiling of a human airway epithelial cell line (Chandrasekaran et al., 2008), human and ferret respiratory tract tissues (Jia et al., 2014; Walther et al., 2013), and porcine airway epithelial cells (Bateman et al., 2010) has revealed the presence of Asn-linked glycans (N-glycans) with extended branches as a unique characteristic of the airway glycome. While the branches of N-glycans on most cell types extend from the mannose core ($Man_3GlcNAc_2Asn$) by a single LacNAc (Galβ1-4GlcNAc) sequence, N-glycans in airway tissues exhibit extensions with multiple LacNAc repeats. Although reports have observed that LacNAc extensions enhance the recognition of human-type receptors by some human influenza HAs, a consistent picture has not yet emerged (Chandrasekaran et al., 2008; Gulati et al., 2013; Nycholat et al., 2012; Yang et al., 2015).

To investigate the importance of this unique feature of glycan structure and to determine its contribution to receptor preference during antigenic drift, we chemo-enzymatically synthesized a series of N- and O-linked glycans extended with one to five LacNAc repeats, and we evaluated the specificity of HAs from H3N2 influenza viruses isolated between 1968 and 2011 using glycan microarrays. We found that recombinant HAs and whole H3N2 viruses exhibit preferential recognition of extended N- and O-glycans terminating in α2-6-linked sialic acids. After 2003, however, a pronounced preference was observed for branched glycans that carry two α2-6 sialic acids and at least three LacNAc repeats. Since little or no binding is observed to the same glycans that terminate with α2-3-linked sialic acids, the basic H3N2 preference for human receptors is maintained. Initially it was thought that selectivity for extended glycan chains exhibited by late H3 isolates might have arisen through steric hindrance by N-glycans added proximal to the HA receptor-binding pocket during antigenic drift, thus limiting the ability of shorter receptors to access the binding site. However, comparison with endoglycosidase-treated H3s, and with the 2009 H1N1 pandemic strain (Cal/04/09), revealed a similar restricted preference for extended, branched N-glycans. We propose that preference for branched glycans may result from increased avidity attained by simultaneous bidentate binding to two HA protomers within an HA trimer.

RESULTS

Preparation of an Influenza Receptor Glycan Microarray with Extended Airway Glycans

Glycan microarray technology has become a widely used tool to rapidly assess the receptor specificity of both HAs and whole viruses (Blixt et al., 2004; Childs et al., 2009; Gulati et al., 2013; Stevens et al., 2006). However, among the glycan arrays available to date, none have systematically covered N-glycans with extended poly-N-acetyl-lactosamine (poly-LacNAc) sequences found in human, swine, and ferret airway tissues. To develop a glycan array library including these structures, we employed an efficient chemo-enzymatic approach to extend poly-LacNAc arms on N- and O-glycan core structures, using *H. pylori* β1-3 N-acetylglucosaminyltransferase (HP β1-3GnT) and mammalian β1-4-galactosyltransferase (GalT-1), followed by capping the terminal galactose residues with sialic acids in either α2-3 or α2-6 linkage, to create an equivalent set of avian-type and human-type receptor analogs (Figure 1A).

The strategy was applied to six O-glycan cores, prepared as previously described (Peng et al., 2012), and to four N-glycan cores, prepared from the sialyl biantennary-N-glyco-hexapeptide (SGP) extracted from egg yolk (Seko et al., 1997) as illustrated in Figures S1A and S1B. The hexapeptide was retained as a linker, since we found that trimming to single β-Asn reduces subsequent printing efficiency on N-Hydroxysuccinimide (NHS)-activated slides (Nycholat et al., 2012). Treatment of SGP with neuraminidase and β-galactosidase yielded 53c, which could be elaborated further to an N-linked core structure containing Fucα1-6GlcNAc (60c) by reaction with fucosyltransferase FUT8 and GDP-Fuc (Ihara et al., 2006). An N-linked core with a third branch (62c) is produced by reaction with N-acetylglucosaminyltransferase GlcNAcT-5 and UDP-GlcNAc (Alvarez-Manilla et al., 2010), and a core with both a third branch and core fucose was produced by reaction with both enzymes (65c) (Figure S1B).

An example of the poly-LacNAc extension is illustrated for the biantennary N-linked Core 53a in Figure S2. Each intermediate with terminal galactose was further sialylated by either rat ST3Gal-III or human ST6Gal-I sialyltransferases to elaborate the sialylated structures with α2-3 or α2-6 sialic acid, respectively. For each step, prior to purification, the reaction mixture was subjected to analysis by mass spectrometry to ensure that no starting material remained. The homogeneous product was obtained by size exclusion chromatography and characterized by nuclear magnetic resonance (NMR) and/or MS analysis. In total, over 70 new sialylated O- and N-glycans were prepared with extended chains comprising one to five LacNAc repeats, as summarized in Figure 1B. Details of the synthesis and characterization of these compounds are provided in the Supplemental Information.

A sialoside glycan array was prepared for analysis of influenza receptor specificity by combining a library of the newly synthesized sialosides with a library of sialylated glycans reported previously (Nycholat et al., 2012; Wang et al., 2013) and printing directly onto NHS-activated glass slides. The resulting sialoside microarray contained 135 glycans, including ten non-sialylated glycans controls (1–10), 69 avian-type sialosides (11–79), and 56 human-type sialosides (80–135) (Table S1). Arrays were subjected to rigid quality control analysis using plant lectins, such as SNA, AAL, and RCA (Figure S3).

Receptor Specificity of HAs from Human H3N2 Viruses, 1968–2011

Several reports document loss of H3 avidity to human-type receptors during antigenic drift, which has been attributed to the

A Generalized Synthesis Scheme

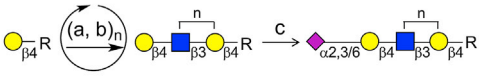

B Poly-LacNAc Extend Sialosides

Glycan Type	Sialoside Symbol Structures	n	Compound number α2,3 Sialosides	Compound number α2,6 Sialosides
O-Linked	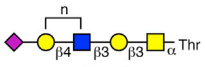 Core 1	1	26	87
		2	27	88
		3	28	89
		4	29	90
		5	30	91
	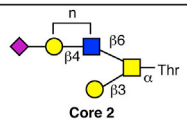 Core 2	1	32	92
		2	33	93
		3	34	94
		4	35	95
		5	36	96
	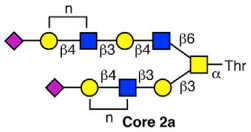 Core 2a	3	37	97
		4	38	98
	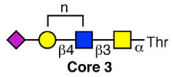 Core 3	1	39	99
		2	40	100
		3	41	101
		4	42	102
		5	43	103
	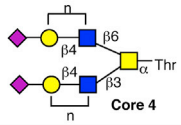 Core 4	1	44	104
		2	45	105
		3	46	106
		4	47	107
		5	48	108
	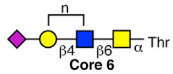 Core 6	4	49	109
		5	50	110
N-Linked	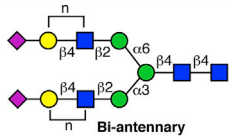 Bi-antennary	1	53	116
		2	56	118
		3	57	120
		4	58	121
		5	59	122
	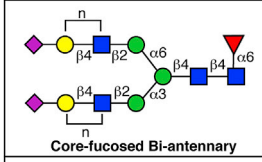 Core-fucosed Bi-antennary	2	NA	123
		3	60	124
		4	61	125
	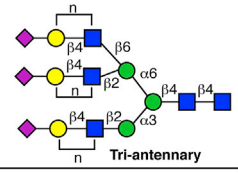 Tri-antennary	2	62	126
		3	63	127
		4	64	128
	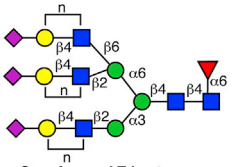 Core-fucosed Tri-antennary	2	65	129
		3	66	130
		4	67	131

Figure 1. Chemo-Enzymatically Synthesized α2-3 and α2-6 Sialosides with Poly-LacNAc Extensions on N-Linked and O-Linked Core Structures

(A) Scheme for the addition of poly-LacNAc structures on N-linked and O-linked glycan core structures. Terminal Gal residues on core structures (R) are iteratively elongated to contain a poly-LacNAc chain using *H. pylori* β1-3 N-acetylglucosaminyltransferase (a) and mammalian β1-4-galactosyltransferase (b, GalT-1). Each compound with terminal galactose is sialylated by either rat ST3Gal-III or human ST6Gal-I sialyltransferases (c) to elaborate the final sialylated structures with α2-3- or α2-6-linked sialic acid, respectively. Synthesis of O-linked and N-glycan core structures are summarized in Figure S1. An example of the poly-LacNAc extension for a biantennary N-glycan is shown in Figure S2.

(B) List of sialosides with poly-LacNAc extended O-linked and N-glycan cores prepared for the glycan array. Compound numbers are used in glycan array figures and throughout the manuscript. See also Figure S3 and Table S1.

accumulation of N-glycosylation that impacts receptor binding, protein folding, and shielding of immunogenic sites (Gulati et al., 2013; Lin et al., 2012; Medeiros et al., 2001; Nobusawa et al., 2000; Skehel et al., 1984; Vigerust et al., 2007) (Table S2). The potential for glycans added near the receptor-binding pocket to impact receptor interactions is illustrated in Figure 2A with a biantennary N-glycan modeled at each confirmed glycosylation site on the HA trimer. To compare the impact of antigenic drift of H3 viruses on receptor avidity and on receptor specificity, we produced representative recombinant HAs spanning 1968–2011 in mammalian cells (293F) (Figure S4).

The avidity of the HAs for simple sialosides was assessed using an ELISA-like assay that was adapted to microarray format by the immobilization of linear NeuAcα2-3diLacNAc ($3SLN_2$-L) or NeuAcα2-6diLacNAc ($6SLN_2$-L) sialosides conjugated to polyacrylamide (PAA) in micro wells of a glass slide (Figure 2B) (McBride et al., 2016; Zhang et al., 2015). All H3 proteins from 1968 to 2003 showed high avidity and specificity to $6SLN_2$, with no apparent binding to $3SLN_2$. By contrast, later H3 proteins, Perth/09 and Vic/11, lost all binding avidity to $6SLN_2$. These results are in agreement with previous reports.

In contrast to the altered binding in the ELISA assay, HAs from 1968 to 2011 all exhibited remarkably similar receptor specificity on the expanded sialoside array, with exclusive binding to α2-6 sialosides (Figure 2C). On further inspection, the earliest HAs bound a broader range of glycans than the later strains. Binding of HAs to linear fragments of larger glycans (83–86) and linear O-glycans (87–91, 99–103, 109, and 110) was most variable, with weakest binding to glycans with only one or two LacNAc (83, 84, 86, 87, 88, 92, 93, 99, and 100). Branched O-glycans with at least three LacNAc repeats were strongly bound by all the HAs (95–98 and 106–108), while glycans with one or two repeats were bound more weakly (92, 93, 104, and 105). Strikingly, the region of the array displaying N-glycans (116–131) exhibited a comb-like appearance for HAs after 1975. The strongest binding was observed to extended glycans with three to five LacNAc repeats in each core series, including biantennary glycans without (120–122) and with (124 and 125) core fucose and triantennary chains both without (127 and 128) or with (130 and 131) core fucose (see Figure 1B). Conversely, in each series, there was relatively poor binding to glycans with two LacNAc repeats (118, 123, 126, and 129), resulting in the gaps and a comb-like appearance. Although one N-glycan with three LacNAc repeats (119) showed less avid binding, this glycan had a single β-Asn

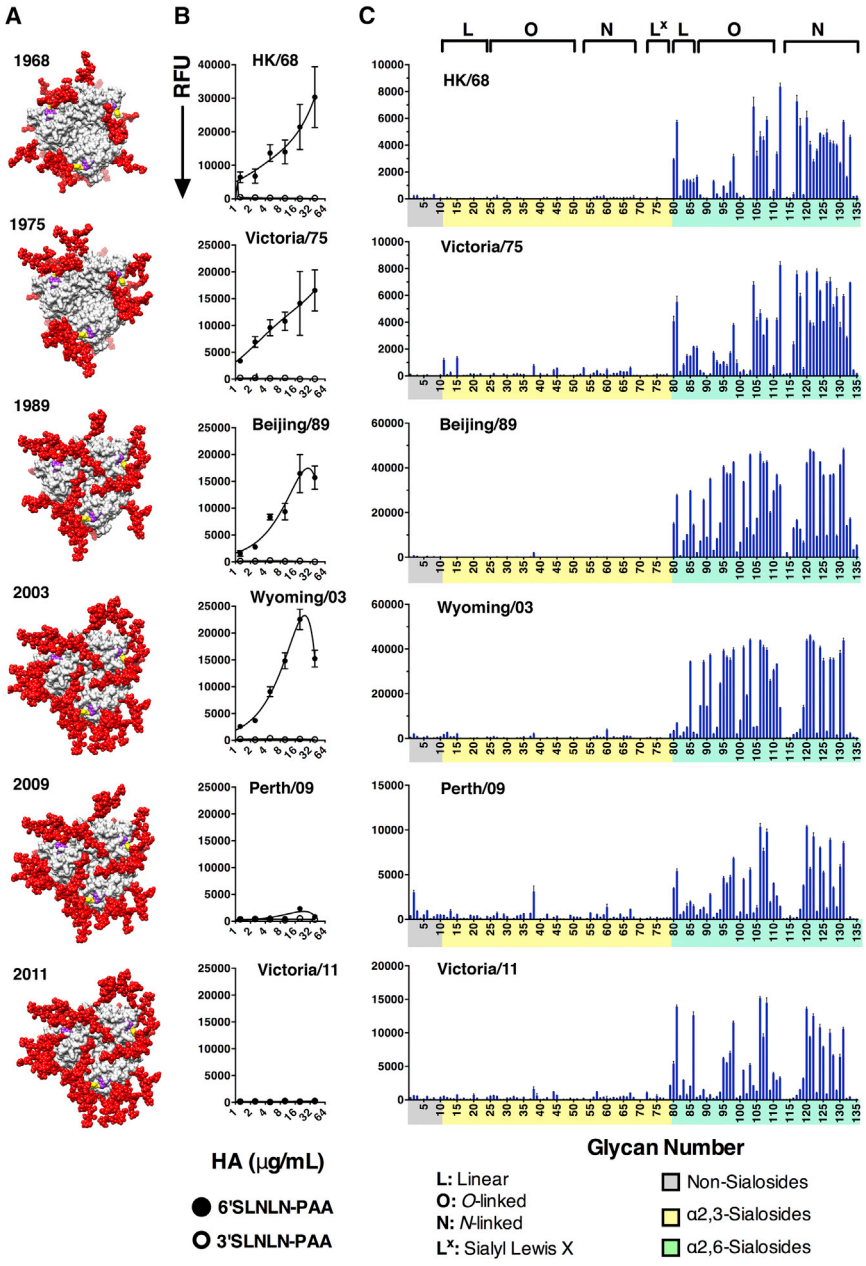

Figure 2. Receptor Specificity of Recombinant H3 Hemagglutinins Spanning 1968–2011

(A) Visualization of the increase in the number of N-glycans that have accrued during H3N2 antigenic drift. A top view of HA is shown with the HA protein in gray with sialic acid (magenta) α2-6 linked to a galactose (yellow) in the receptor-binding site of each protomer of the trimer. Asialo-LacNAc-biantennary-N-glycans (red spheres) are modeled at each known glycosylation site on the HA surface (see also Figures S4 and S5 and Table S2). Strain-specific glycosylation sites are modeled onto the structure of Vic/11 H3 in each case.

(B) H3 isolates isolated after 2009 lose avidity to polyacrylamide (PAA) conjugates bearing NeuAcα2-3diLacNAc ($3SLN_2$, open circles) or NeuAcα2-6diLacNAc ($6SLN_2$, closed circles) glycans. These PAA-glycans were imprinted in a multi-well microarray and overlayed with serially diluted HA (1.3–40 μg/mL). After washing, bound HA was detected with mouse anti-HIS- and AlexaFluor488-labeled anti-mouse-IgG as described in the Experimental Procedures.

(C) Recombinant H3 HA proteins exhibit specificity for a subset of human-type receptors. Glycans on the array comprise non-sialoside controls (1–10; gray), α2-3 sialosides (11–79; yellow), and α2-6 sialosides (80–135; green). Glycans are grouped by structure type (see top): L, linear; O, O-linked; N, N-linked; and L^x, sialyl Le^x (see also Table S1). Signals are the mean and SE calculated for six independent replicates on the array after removal of the highest and lowest signals.

linker that had reduced coupling to the NHS-activated slides compared to the hexapeptide linker of the other N-glycans (118 and 120–131). In summary, despite the apparent loss of avidity of H3 after 2003, these HAs maintained binding to extended, branched N- and O-glycans on the array, providing evidence of conserved receptor specificity during almost 50 years of antigenic drift.

Comparison with Previous Specificity Results of 2006–2007 H3N2 Viruses

Previous glycan array analysis of influenza viruses isolated in 2006 and 2007 reported widely varying receptor specificity for different isolates and inconsistent preference for human-type α2-6 sialosides (Gulati et al., 2013; Stevens et al., 2010). Using aliquots of eight of the same viruses that were isolated from respiratory secretions and produced in MDCK cells, we evaluated receptor specificities on the expanded array (Figure 3). It was apparent that these viruses have a very similar binding pattern compared to one another and to recombinant H3 HAs (Figure 2). All H3N2 viruses consistently bound to branched α2-6 sialosides with three to five LacNAc repeat unit extensions, including, for most viruses, the comb-like pattern resulting from reduced binding to di-LacNAc extended glycans for each N-glycan core (116–131).

These results are in contrast to glycan array analyses reported previously for the same viruses (Stevens et al., 2010), where it was concluded that there was no consistent receptor specificity and that some viruses bound preferentially or equally to α2-3 sialosides. In light of data presented here, this discrepancy now clearly resulted from a lack of extended receptors on previously available glycans arrays (Figure 1B). Our expanded array library also features glycans employed in these earlier studies that are shown in red in Figure 3. Looking at the red highlighted signals, it is apparent that binding to these receptors was weak relative to the robust binding to extended α2-6 sialylated glycans. Moreover, if the highlighted red signals in Figure 3 are normalized to full

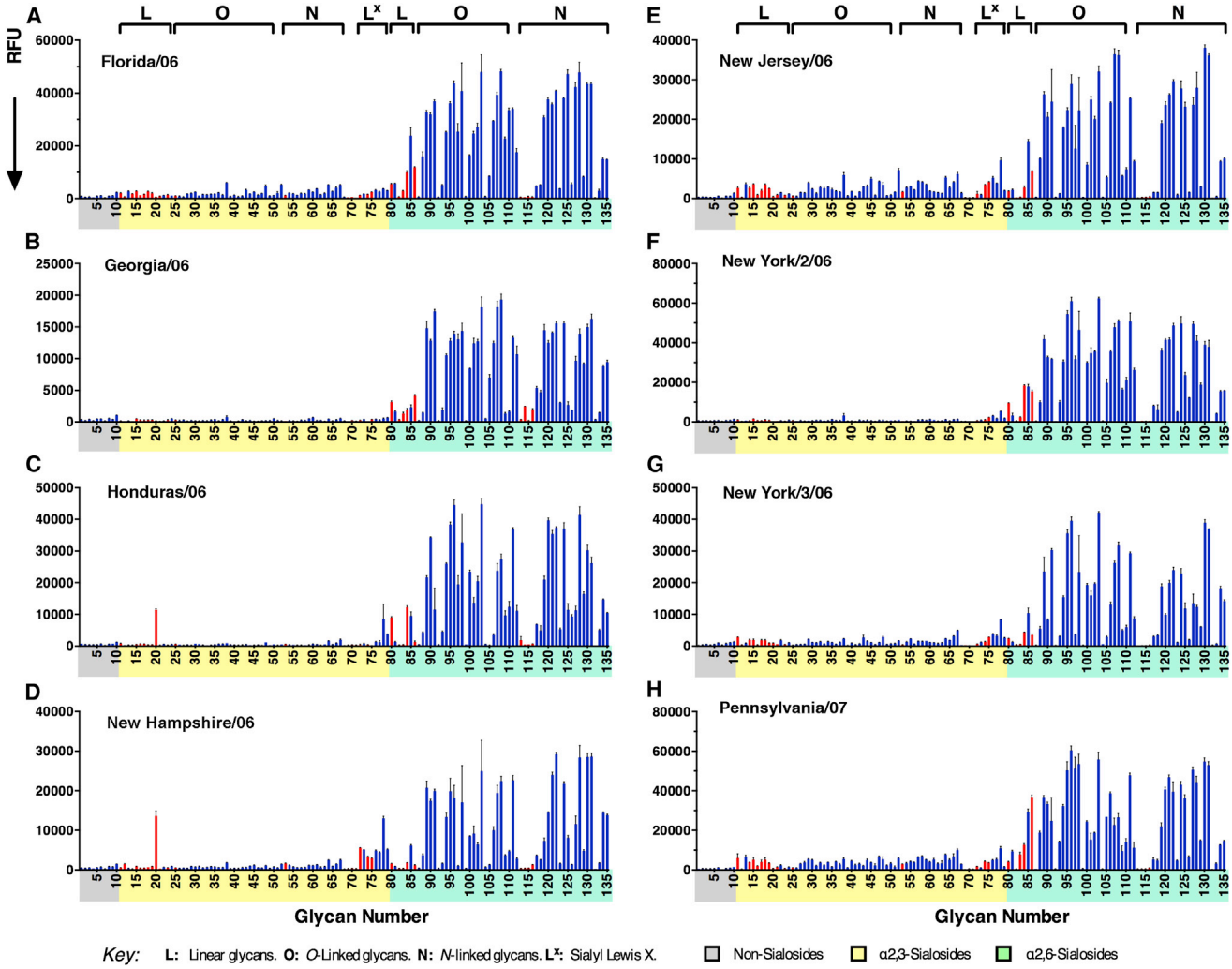

Figure 3. Receptor Specificity of 2006/2007 Human Influenza A H3N2 Viruses

(A–H) Intact H3N2 viruses exhibit consistent human-type receptor specificity on the expanded sialoside array. Viruses tested were from frozen aliquots of human influenza isolates grown on MDCK cells Florida/06 (A), Georgia/06 (B), Honduras/06 (C), New Hampshire/06 (D), New Jersey/06 (E), New York/2/06 (F), New York/3/06 (G), and Pennsylvania/07 (H), and they were identical to those previously found to have varied specificity on a glycan array without poly-LacNAc extended N-linked and O-linked glycans (Stevens et al., 2010). The signals highlighted in red correspond to the glycan structures on the microarray used in the previous study. See also Table S1.

Signals are the mean and SE calculated for six independent replicates on the array after removal of the highest and lowest signals.

scale (as normally done in array experiments) and only these signals are considered in assigning receptor specificity, specificity of the various viruses does indeed appear varied as reported previously (Stevens et al., 2010). However, on this expanded array that includes glycans with extended glycan chains, the receptor specificities of the viruses are remarkably similar.

Specificity of H5N1, Avian H3N8, Human H3N2, and Pandemic H1N1 HAs

To place the preference of H3 HAs for extended α2-6 sialosides into a broader context, we compared receptor specificities from an H5N1 virus (A/VN/1203/04, isolated from human but with avian-type receptor specificity), the avian H3 pandemic progenitor virus (A/Duck/UKR/63 [H3N8]), a human 2010 H3N2 virus sequenced directly from the clinical isolate without prior growth in laboratory hosts (A/HK/6934/10), and the H1N1 2009 pandemic virus (A/Cal/04/09) (Figure 4). The H5 and avian H3 progenitor HAs recognized only α2-3 sialosides, with a preference for branched N- and O-glycans and little selectivity for length, thus confirming that the specificity of these avian viruses is maintained across a diverse range of glycans (Figures 4A and 4B). In contrast, the 2010 H3N2 clinical isolate exhibited the most restricted specificity, binding exclusively to branched N- and O-linked α2-6 sialosides (Figure 4C).

The 2009 H1N1 pandemic virus Cal/04/09 is well documented to exhibit low avidity in receptor-binding assays, precluding analysis of receptor specificity on glycan microarrays due to inefficient binding (Stevens et al., 2010). Remarkably, on this expanded array, Cal/04/09 HA exhibited robust and restricted binding to extended, branched α2-6 sialosides with preference

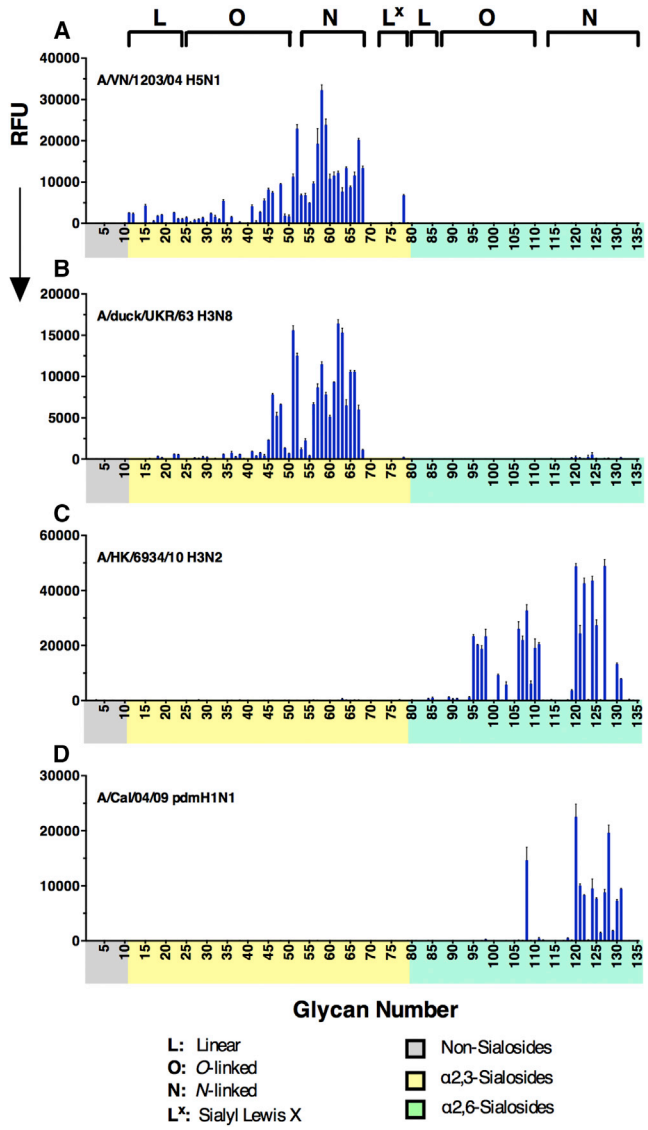

Figure 4. Receptor Specificity of HA Proteins from a Human H5N1 Infection, an Avian H3N8, a Clinical H3N2 Isolate, and 2009 Pandemic H1N1

(A and B) Glycan microarray analyses of (A) recombinant H5 HA from A/Vietnam/1203/04 H5N1 and (B) an avian H3 precursor to the 1968 human pandemic strain (A/Duck/Ukraine/1/1963 [H3N8]) show typical avian-type specificity for α2-3 sialosides.

(C and D) Glycan microarray analyses of (C) recombinant H3 from an A/HK/6934/2010 (H3N2) patient isolate and (D) H1 Cal/04/09 HA show binding almost exclusively to N-glycans with three or more LacNAc repeats.

Signals are the mean and SE calculated for six independent replicates on the array after removal of the highest and lowest signals.

for N-glycans with three or more LacNAc repeats (120–122, 124, 125, 127, 128, 130, and 131) and a single branched O-glycan with five LacNAc repeats (108). Thus, as exemplified by the H3 HAs (Figures 2 and 3) and this low-avidity 2009 pandemic virus (Figure 4D), human influenza HAs consistently bind branched N- and O-glycans with three or more LacNAc repeats with higher avidity than linear glycans and branched glycans with shorter chains.

Extended Glycan Receptors Increase Avidity and Support H3N2 Infection of MDCK Cells

To directly assess the biological impact of glycan length, we coupled linear and N-glycans with one to four LacNAc repeats to biotin for ELISA-type assays and to lipids to assess their ability to serve as receptors for virus infection in MDCK cells (Figure 5A). The avidity of H3 HAs from HK/68 and Vic/11, representative of early and late strains, was assessed by overlaying purified HA onto biotinylated glycans adsorbed to streptavidin-coated plates. For HK/68 H3, binding to linear glycans ($6SLN_{1-4}$-L) was weak and had little dependence on glycan length. Binding to shorter branched N-glycans ($6SLN_{1-2}$-N) showed similarly low avidity to linear receptors, while binding to longer N-glycans ($6SLN_{3-4}$-N) was dramatically stronger (Figure 5B, left). In contrast, for Vic/11 HA, binding was strongly dependent on glycan length for both linear and branched N-glycans. Indeed, there was no detectable binding to shorter receptors ($6SLN_{1-2}$-L and $6SLN_{1-2}$-N) over the avian virus receptor control ($3SLN_2$-L), and there was strong binding to longer glycans ($6SLN_{3-4}$-L and $6SLN_{3-4}$-N), amounting to >100-fold higher avidity relative to the non-binding shorter glycans (Figure 5B, right).

To assess the length dependence of sialosides as receptors for infection, we reasoned that MDCK cells could be engineered to carry synthetic sialoside receptors coupled to lipid anchors that would spontaneously insert into the cell membrane, as shown for glycolipid receptors of Sendai virus (Markwell and Paulson, 1980; Markwell et al., 1981). To this end, MDCK cells were treated with *C. perfringens* neuraminidase (CPN) to destroy endogenous receptors, overlaid with lipid-conjugated glycans, and incubated briefly with low-titer virus samples. After washing, bound viruses were allowed to replicate for 48 hr and final titers were assessed by plaque assay. For both HK/68 and Vic/11, CPN pre-treatment of cells effectively abolished susceptibility to infection, while cells treated with the lipid-linked avian-type receptor ($3SLN_3$) produced no virus. However, for HK/68, susceptibility to infection was fully restored by lipid-linked human-type receptor glycans ($6SLN_{1-3}$-L and $6SLN_{1-3}$-N) regardless of length (one to three LacNAc repeats) or branching (Figure 5C, left). In contrast, for Vic/11, susceptibility to infection was restored more selectively, with strong preference for longer glycans. For the linear series, $6SLN_3$-L restored replication equivalent to native MDCK cells, with $6SLN_2$-L somewhat less, and the virus did not replicate with $6SLN_1$-L (Figure 5C, right). For the biantennary N-glycans, only the longest human-type receptor ($6SLN_3$-N) restored replication, recapitulating the binding activity results of the ELISA assays and glycan arrays.

Preference for Extended, Branched N-Linked Receptors Is Not Due to the HA Glycan Shield

One possible explanation for the striking preference of the exemplary Vic/11 HAs for extended glycan receptors is that they are of sufficient length to allow the sialic acid to reach the receptor-binding site without being sterically restricted by N-glycans added around the HA receptor-binding site. To directly assess this possibility, we expressed the A/Vic/11 and A/HK/68 HAs in HEK293S cells that produce only high mannose glycans, allowing them to be removed by treatment with endoglycosidase H

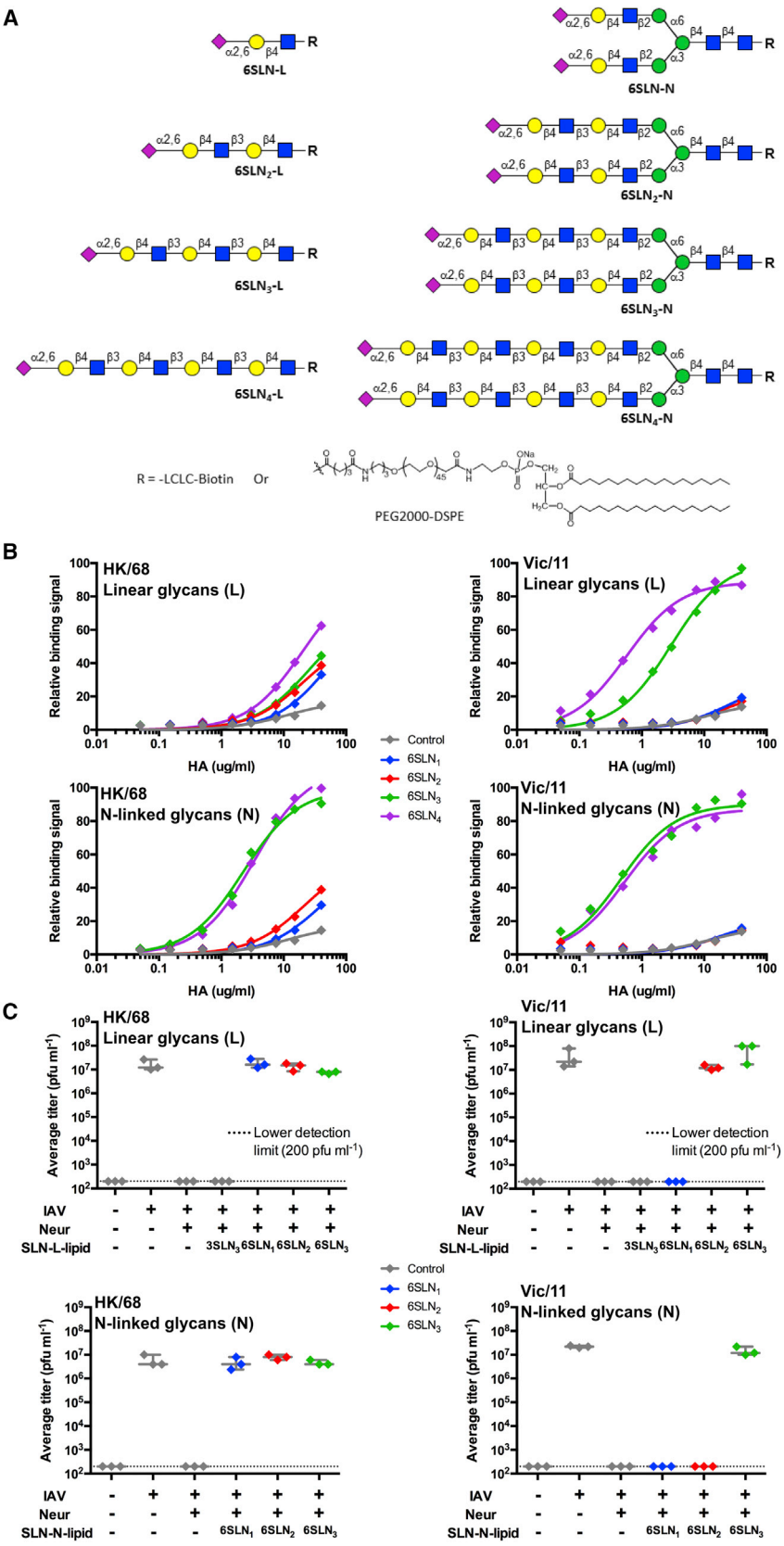

Figure 5. Glycan Binding Specificity of H3N2 HK/68 and Vic/11 for Host Cell Receptors

(A) The α2-6 sialosides with one to four LacNAc extensions used in the ELISA analysis of HA-binding specificity (biotinylated glycans) or virus infection study (lipidated glycans) are shown. L, linear glycans; N, N-glycans.

(B) ELISA analysis of H3N2 HK/68 (left) and Vic/11 (right). HK/68 HA shows weak binding to all linear α2-6-sialosides regardless of length, and it binds preferentially to branched N-glycans with tri- and tetra-LacNAc extensions. Apparent K_d for each glycan was calculated using the Prism 6 software package ($6SLN_3$-N = 1.83 ± 0.16 μg/mL and $6SLN_4$-N = 2.09 ± 0.22 μg/mL). Vic/11 HA shows specificity toward α2-6 receptors with tri- and tetra-LacNAc extensions both in linear and N-glycan structures. K_d for respective glycans were as follows: $6SLN_3$-L = 2.95 ± 0.21 μg/mL, $6SLN_4$-L = 0.57 ± 0.04 μg/mL, $6SLN_3$-N = 0.46 ± 0.05 μg/mL, and $6SLN_4$-N = 0.53 ± 0.07 μg/mL. Linear, biotinylated NeuAcα2-3diLacNAc ($3SLN_2$-L) was used as a negative control (gray diamonds) in all experiments.

(C) Infection of glycolipid-engineered MDCK cells (linear and N-linked) with both HK/68 (left) and Vic/11 (right) H3N2 viruses. Plots are average virus titers, measured by plaque assay, at 48 hr post-infection (HPI). From left to right in each panel, MDCK monolayers were treated with PBS only (mock infected), 50–80 PFUs virus (positive control), CPN then 50–80 PFUs virus (background), or treated with CPN, overlaid with SLN-glycolipids, then virus. Linear NeuAcα2-3triLacNAc ($3SLN_3$-L) glycolipid was used as a negative control (gray diamonds). See also Figure S7.

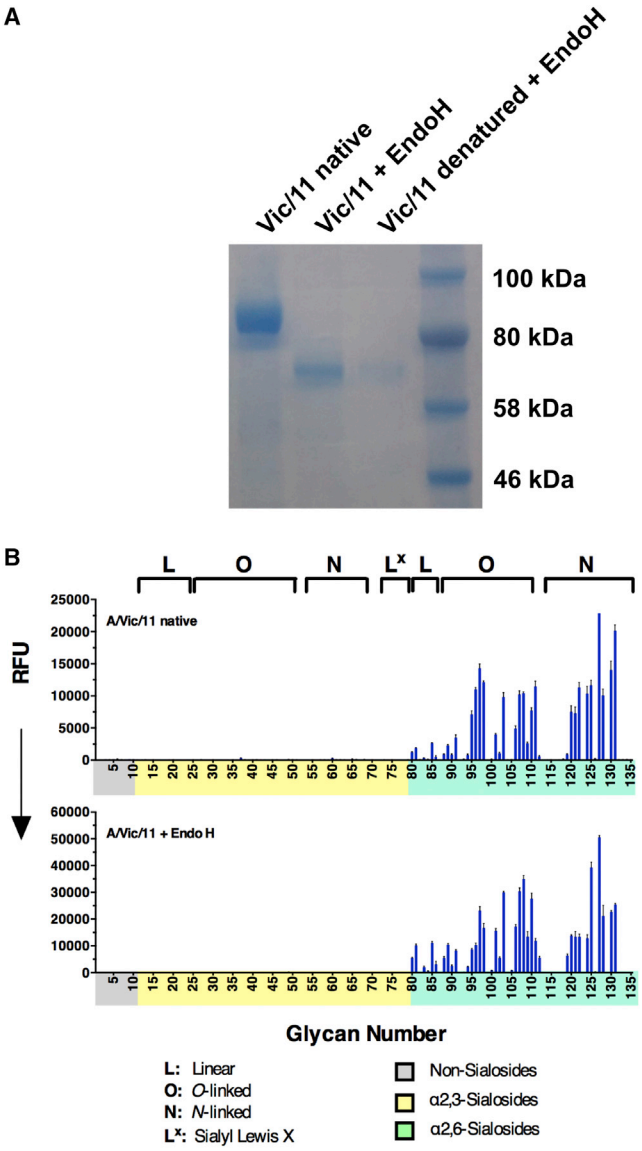

Figure 6. HA Deglycosylation Does Not Restore Binding to Shorter Glycan Receptors in Vic/11

(A) Vic/11 HA was expressed in 293S cells (left) and natively deglycosylated using Endo H (center). As a control, a small HA sample was denatured prior to Endo H treatment (right) to ensure complete deglycosylation of the folded protein.

(B) Receptor specificities of glycosylated (upper) and Endo H-treated (lower) Vic/11 HA were analyzed by glycan microarray. See also Figure S7.

Signals are the mean and SE calculated for six independent replicates on the array after removal of the highest and lowest signals.

(Endo H). As shown in Figure 6A, Endo H removed the glycans efficiently, yielding an apparent molecular weight (63.2 kDa) equivalent to that of Endo H-treated HK/68 HA (Figure S7A). Remarkably, glycan arrays showed no change in specificity as a result of deglycosylation (Figures 6B and S7B). In particular, Vic/11 maintained its extreme preference for human-type branched N-glycans with at least three LacNAc repeats, resulting in the familiar comb-like appearance for binding to N-glycans 115–131.

Molecular Dynamics Simulation of Bidentate Binding of an N-Glycan to an HA Trimer

It is striking that H3 HAs from 1989 to 2011 and the Cal/04/09 H1 HA bind with higher avidity to branched, extended N-glycans with more than two LacNAc repeats. Since this specificity does not appear to be sensitive to the presence of HA N-glycans, we considered that the extended, branched glycans could adopt a unique geometry that permits simultaneous bidentate binding to receptor sites on two protomers within the same HA trimer, which are ~45 Å apart (Figures 7A and 7B). To assess this possibility, 3D structures for biantennary glycans were generated and grafted (Nivedha et al., 2014) onto the bound receptor oligosaccharide in a crystal structure of HA (CA/04/09; PDB: 3UBE), such that the NeuAcα2-6Gal receptor fragment was constrained to bind in the same conformation in the reported structure (Grant et al., 2016; Xu et al., 2012). NeuAcα2-6Gal on the other arm of the glycan was then brought toward the binding site of an adjacent protomer by varying the intervening glycosidic linkages within normal angular bounds (Nivedha et al., 2014). Structures that were closest to displaying bidentate binding were subsequently refined using molecular dynamics simulation. Modeling data showed that SLN_2 glycans were too short to form bidendate complexes (Figure 7C), whereas longer glycans with SLN_3, SLN_4, and SLN_5 extensions were capable of adopting low-energy shapes that permitted simultaneous binding of the two arms, as illustrated for SLN_3 in Figure 7D (see also Movies S1, S2, S3, and S4). It is notable that attempts to simultaneously dock both branches of a biantennary SLN_5 glycan terminating with the NeuAcα2-3Gal linkage failed to generate bidentate complexes.

Modeling also confirmed the potential for bidentate binding to the HA of glycosylated H3N2 viruses. To generate an ensemble of conformations, molecular dynamics (MD) simulations for a glycosylated model of an H3 (Vic/11; PDB: 4O5N) trimer with asialo-LacNAc-biantennary-N-glycans at positions N165 and N246 were performed. Although some conformations of glycans at N165 and N246 led to clashes with a bound bidentate receptor glycan, orientations of glycans at N165 and N246 were identified that tolerated bidentate binding (see Figure S5).

The results confirm the ability of extended (SLN_3 or longer) branched glycans to form bidentate complexes with either glycosylated or non-glycosylated H3 HAs. Bidentate binding would increase the avidity of the glycan-HA binding, consistent with the comb-like binding pattern in the glycan array data (Figures 2, 3, and 4).

DISCUSSION

Despite reports that evolution of the human H3N2 virus has been accompanied by diminished recognition of human-type receptors (Gulati et al., 2013; Yang et al., 2015), we find that the virus has maintained consistent specificity for a subset of branched human-type receptors that have sialic acid α2-6 linked to poly-LacNAc extended glycans, with little or no binding to the same glycans with α2-3 sialic acids. Although the preference for longer glycans has become exaggerated over time and coincides with the acquisition of additional glycans around the receptor-binding pocket during antigenic drift, we show here that restricted specificity of the recent H3 isolates is unrelated to the steric clash of

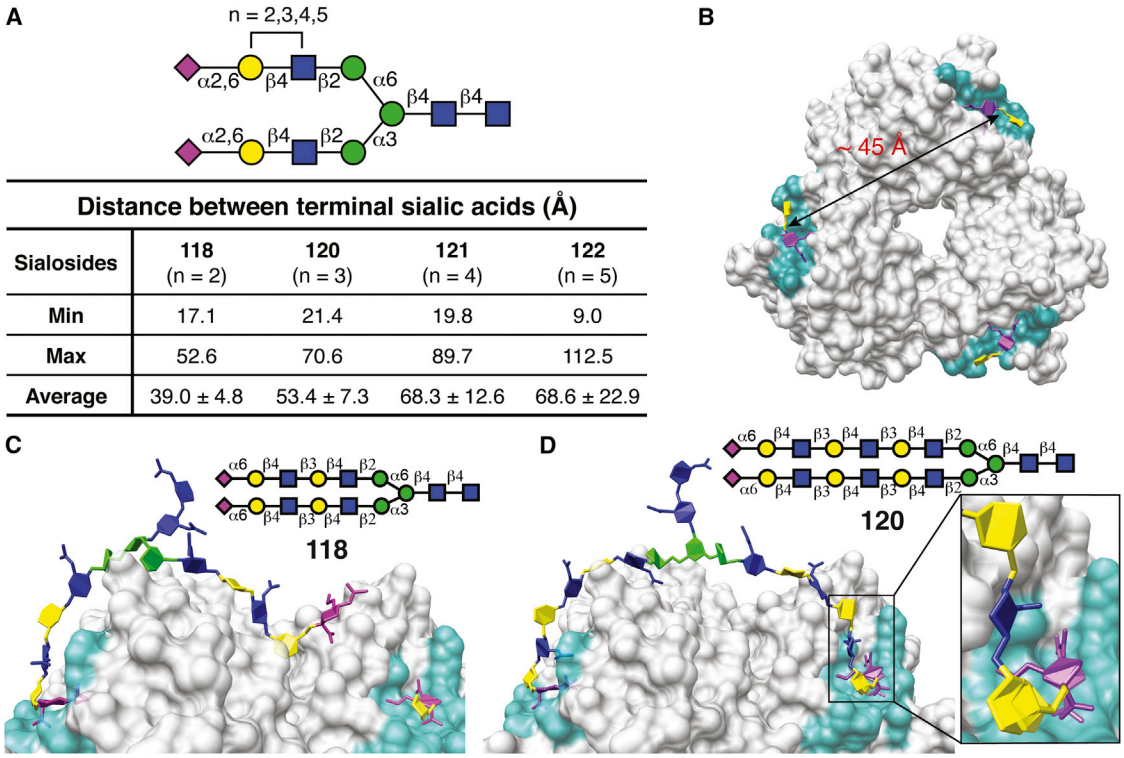

Distance between terminal sialic acids (Å)

Sialosides	118 (n = 2)	120 (n = 3)	121 (n = 4)	122 (n = 5)
Min	17.1	21.4	19.8	9.0
Max	52.6	70.6	89.7	112.5
Average	39.0 ± 4.8	53.4 ± 7.3	68.3 ± 12.6	68.6 ± 22.9

Figure 7. Proposed Model of Bidentate Binding of N-glycans into the H1 Cal/04/09 HA Trimer

(A) Summary of the distances between the C2 atoms in the sialic acids in each arm of each biantennary N-glycan is shown (see Figure S6 for triantennary sialosides).

(B) The distance between the C2 atoms of the sialic acid in two binding sites (cyan) of the HA1 head group trimer. Bound disaccharide ligands (NeuAcα2-6Gal) are shown in sticks (magenta/yellow).

(C) The di-LacNAc sialoside 118 is incapable of bivalent binding to two receptor-binding sites within a Cal/04 HA trimer.

(D) The tri-LacNAc sialoside 120 is capable of spanning the distance between two receptor-binding sites within an H1 Cal/04/09 HA trimer. Inset: the sialic acid of the biantennary N-glycan adopts the same conformation as the receptor glycan (NeuAcα2-6Gal) in the crystal structure (see also Movies S1, S2, S3, and S4 and Figure S5 for a top view of the H3 HA trimer in complex with sialoside 120).

glycans added to the HA (Figure 6). We suggest that the strong preference for branched longer-chain glycans of the receptor can result from the potential to increase avidity by binding to two protomers of the same HA trimer. It appears that the enhanced specificity of late H3N2 isolates is largely due to a process of avidity maturation, where H3 HAs are evolving a binding mode favoring multivalent receptor interactions and simultaneously losing specificity for shorter, linear receptors incapable of supporting these contacts.

N-glycans used in our array here are observed in respiratory tissue of different influenza-susceptible species including humans. Although the requirement for N-glycans in cell-based experiments is still unclear (Chu and Whittaker, 2004; de Vries et al., 2012), it is remarkable that the extended biantennary N-glycans linked to lipids could by themselves restore infection to receptor-deficient MDCK cells. Clearly, they are sufficient to mediate binding of the virus to the surface of the cell; however, we know that sialic acids are replaced on the surface of neuraminidase-treated cells within hours of treatment. Thus, it remains to be seen if the lipid-linked glycans mediate binding only or both binding and endocytosis of the virus.

Here we also provide evidence that branched N-glycans with at least three LacNAc repeats are capable of forming bidentate binding with their sialic acid termini, where two branches can bridge the binding sites of two protomers on the same HA trimer. This binding mode effectively increases avidity, and it is particularly relevant to the human 2009 pandemic Cal/04/09 H1N1 virus, which has the strictest specificity for branched N-glycans (Figure 4D). In this context, it is notable that the NeuAcα2-6Gal linkage has a preferred low-energy solution conformation of the terminal tri-saccharide that allows NeuAcα2-6Galβ1-4GlcNAc to project the glycan chain up over the 190 helix toward the top of HA (Chandrasekaran et al., 2008), and, as a consequence, positions the rest of the glycan at the apex of the trimer, allowing the other branch to bridge to the receptor-binding site of an adjacent HA subunit (Figure 7; Movies S1, S2, S3, and S4).

In this report, observations of H3 HA binding to a series of structurally related glycans in different assays and use of an expanded glycan array provide relevant insights into ambiguous receptor specificity analyses from previous studies. For recent H3 isolates, it is evident that shorter glycans cannot reliably be used to assess receptor specificity, since the binding mode over the evolution of H3N2 from 1968 to present day favors receptors with extended glycans without any change in specificity for human-type receptors. We and others have shown that historic H3N2 strains bind to linear α2-6 sialylated glycans (Gulati

et al., 2013; Lin et al., 2012; Yang et al., 2015). However, after 2003, H3 HAs appear to exhibit relatively weak and inconsistent binding to linear glycans, even when featuring up to five LacNAc repeats (e.g., glycans 83–85 and 87–91). However, N-glycans with three or more LacNAc units exhibit robust and reproducible binding to all H3s tested (Figures 2, 3, and 4).

While these observations fully support our proposed model of bidentate binding, factors other than glycan structure can influence binding avidity. For instance, in the glycan array, the linear glycans are coupled to the array surface with a short linker (ethanolamine), while the N-glycans are further extended from the array surface by the Man_3GlcNA_2 core and a hexapeptide linker. In the ELISA assay, the same glycans are uniformly coupled to longer biotinylated linkers (LCLC-biotin) bound to streptavidin. Here, linear glycans featuring four LacNAc repeats exhibit comparable avidities to N-linked counterparts when binding to Vic/11 HA. In infectivity assays, glycans are attached to lipid via a 2000 MW PEG linker, dramatically extending distance from the surface again. In this format, linear glycans now with only two or three LacNAc repeats are able to restore infectivity to receptor-deficient MDCK cells. Converse to this apparent linear variability, in all three assays, length dependence for biantennary N-glycans is far more strongly conserved, with three or more LacNAc repeats required for binding. This suggests that, for receptors featuring multiple antennae, the length of the glycan arm relative to its attachment to the branching core is what is important, and extending the linker has no additional impact.

Although glycomic profiling of an airway epithelial cell line (Chandrasekaran et al., 2008), human and ferret respiratory lung tissues (Jia et al., 2014; Walther et al., 2013), and swine respiratory epithelium (Bateman et al., 2010) suggests the presence of extended, branched N-glycans similar to those studied here, definitive analysis of human airway epithelium and, in particular, different sections of the airway still remains to be carried out. A recent report suggesting that the soft palate of ferrets plays a prominent role in the selection of HA mutations that promote a switch from avian-type to human-type receptor specificity (Lakdawala et al., 2015) emphasizes how potential variation in the expression of receptor glycans in different regions of the upper airway could account for selection of viruses with specificity for extended human-type receptors. Clearly, additional information on the types of glycans expressed along the human airway epithelium will help refine our understanding of selective pressures that maintain human-type receptor specificity in human influenza viruses and the role of receptor binding as a barrier for the emergence of new pandemic viruses from avian and other animal influenza viruses.

The practical implications of these findings extend to the difficulty of isolating and propagating recent H3N2 viruses for the production of vaccines (Asaoka et al., 2006). It is well documented that the propagation of primary isolates in MDCK cells and eggs is difficult, and it often results in mutations in the HA and neuraminidase (NA) that compensate for weak binding of the virus to receptor glycans found in those hosts (Hardy et al., 1995; Lee et al., 2013; Nobusawa et al., 2000). When the problem for isolation of virus in MDCK cells was first recognized, MDCK cells engineered to contain a higher density of human-type receptors were found to improve recovery of virus from human samples (Oh et al., 2008; Hatakeyama et al., 2005). Knowledge that recent H3N2 viruses prefer extended, branched glycan receptors provides a further rational basis to identify or engineer laboratory hosts that contain receptors favorable for binding of human influenza viruses.

EXPERIMENTAL PROCEDURES

Synthesis of Glycans

Glycan core structures were prepared as previously described (Peng et al., 2012). The poly-LacNAc chains were obtained by chemo-enzymatic extension using *H. pylori* β1,3-GlcNAcT and mammalian GalT-1, subsequently followed with sialylation by either hST6Gal-I or rST3Gal-III (Figure 1A). Full details of all synthesis steps are included in the Supplemental Experimental Procedures.

Glycan Array Printing and Quality Control

Glycan arrays were custom printed on a MicroGridII (Digilab) using a contact microarray robot equipped with StealthSMP4B microarray pins (Telechem), as previously described (Xu et al., 2012). Briefly, samples of each glycan were diluted to 100 μM in 150 mM Na_3PO_4 buffer (pH 8.4). Aliquots of 10 μl were loaded in 384-well plates and imprinted on NHS-activated glass slides (SlideH, Schott/Nexterion), each containing six replicates of each glycan. Remaining NHS-ester residues were quenched by immersing slides in 50 mM ethanolamine in 50 mM borate buffer (pH 9.2) for 1 hr. Blocked slides were washed with water, centrifuged dry, and stored at room temperature until use.

Expression and Purification of Recombinant HA

Recombinant H3 subtype HAs from 1968 to 2011 viral isolates, A/HK/1/68 (HK/68), A/Victoria/3/77, A/Beijing/353/89, A/Wyoming/3/03, A/Perth/16/09, and A/Victoria/361/11 (Vic/11), were expressed in 293F freestyle expression system as described previously (Lee et al., 2014). H1 A/Cal/04/09 (Cal/04/09), H3 A/HK/6934/10, H3 A/Duck/UKR/63, and H5 A/VN/1203/04, and for some experiments Vic/11, HAs were expressed in HEK293S ($GnTI^{-/-}$) cells and purified from the cell culture supernatants as described previously (de Vries et al., 2013).

Preparation of H3N2 Viruses

The H3N2 viruses used in this study, A/Florida/2/06, A/Georgia/4/06, A/Honduras/3112/06, A/New Hampshire/3/06, A/New Jersey/2/06, A/New York/2/06, A/New York/3/06, A/Pennsylvania/4/07, and Vic/11, were obtained from the Centers for Disease Control and Prevention (CDC) and the CDC-Influenza Reagent Resource (CDC-IRR). They were grown in MDCK cells, purified, and frozen in aliquots for glycan array analysis, as previously described (Stevens et al., 2010).

Glycan Array Analysis Experiments

Purified, soluble trimeric HA (50 μg/mL) was pre-complexed with either an anti-HIS or anti-Strep mouse antibody and an Alexa647-linked anti-mouse IgG was added (4:2:1 molar ratio) for 15 min on ice in 100 μL PBS-T; this was incubated on the array surface in a humidified chamber for 90 min. Array analysis of inactivated virus stocks was performed as described previously (Stevens et al., 2010).

ELISA with Biotinylated Glycans

For glycan ELISA, purified HA trimers were concentrated to 500 μg/mL, pre-complexed with anti-HIS mouse antibody and HRP-conjugated anti-mouse IgG, then diluted in series to appropriate assay concentrations (typically 40–0.05 μg/mL final). Preparation of streptavidin-coated plates with biotinylated glycans, incubation, and washing of pre-complexed HA dilutions was exactly as previously described (Chandrasekaran et al., 2008).

Virus Infection Study

MDCK cells were grown to confluency in six-well tissue culture trays and digested with 50 units (per well) of commercial CPN (New England BioLabs). Cells were then incubated with 3 μM (final) glycolipid ($6SLN_{1-3}$-L/N lipid) for 20 min, followed by 50–80 plaque-forming units (PFUs) virus for 10 min. Bound virus was allowed to grow for 48 hr at 37°C, with final solution titers assessed by plaque assay. Full virus infection protocols are described in the Supplemental Experimental Procedures.

Molecular Modeling

For 3D structure generation, initial conformations for biantennary α2-6 di-, tri-, tetra-, and penta-LacNAc glycans were built and energy minimized using GLYCAM-Web (http://www.glycam.org). The trimeric HA1 domains of H1 Cal/04/09 and H3 Vic/11 were generated from PDB: 3UBE and 4O5N, respectively. For complexes, each N-glycan receptor was grafted into an HA-binding site by superimposing the NeuAcα2-6Gal-binding motif of one branch onto the crystal structure of the ligand bound to the HA. Structures were then refined and energy minimized to assess the ability of the sialic acid on the other branch to reach the binding site of another protomer. Details are provided in the Supplemental Experimental Procedures.

SUPPLEMENTAL INFORMATION

Supplemental Information includes Supplemental Experimental Procedures, seven figures, two tables, and four movies and can be found with this article online at http://dx.doi.org/10.1016/j.chom.2016.11.004.

AUTHOR CONTRIBUTIONS

W.P., R.P.d.V., I.A.W., R.J.W., and J.C.P. designed the project. W.P. synthesized glycans and biotinylated and lipidated sialosides. B.T. assisted in synthesis of glycans. N.R. assisted in the expression of glycosyltransferases. R.P.d.V., A.J.T., and P.S.L. expressed recombinant proteins. R.M. produced glycan arrays. W.P., R.P.d.V., A.J.T., R.M., and J.C.P. analyzed glycan array data. O.C.G. performed molecular modeling. A.J.T. performed glycan ELISA and virus infection study. W.P., R.P.d.V., and J.C.P. wrote the manuscript and all authors reviewed and edited the manuscript.

ACKNOWLEDGMENTS

This work was funded in part by grants from the NIH (AI114730 to J.C.P., CA207824 and GM103390 to R.J.W., and R56 AI117675 to I.A.W.) and the Kuang Hua Educational Foundation (to J.C.P.). R.P.d.V. is a recipient of Rubicon and VENI grants from the Netherlands Organization for Scientific Research (NWO). A.J.T. is the recipient of a Long-term Fellowship from the European Molecular Biology Organization (EMBO ALTF 963-2014). We thank Li-Mei Chen and Ruben Donis of the Centers for Disease Control for samples of 2006 H3N2 viruses, Jennifer Pranskevich for preparation of enzymes used in the synthesis of glycans, and Anna Crie for help in the preparation of figures and tables. The Consortium for Functional Glycomics (http://www.functionalglycomics.org/) funded by NIGMS grant GM062116 (J.C.P.) provided several glycans used in this study.

Received: November 10, 2015
Revised: July 27, 2016
Accepted: November 7, 2016
Published: December 22, 2016

REFERENCES

Alvarez-Manilla, G., Troupe, K., Fleming, M., Martinez-Uribe, E., and Pierce, M. (2010). Comparison of the substrate specificities and catalytic properties of the sister N-acetylglucosaminyltransferases, GnT-V and GnT-Vb (IX). Glycobiology *20*, 166–174.

Asaoka, N., Tanaka, Y., Sakai, T., Fujii, Y., Ohuchi, R., and Ohuchi, M. (2006). Low growth ability of recent influenza clinical isolates in MDCK cells is due to their low receptor binding affinities. Microbes Infect. *8*, 511–519.

Bateman, A.C., Karamanska, R., Busch, M.G., Dell, A., Olsen, C.W., and Haslam, S.M. (2010). Glycan analysis and influenza A virus infection of primary swine respiratory epithelial cells: the importance of NeuAcα2-6 glycans. J. Biol. Chem. *285*, 34016–34026.

Blixt, O., Head, S., Mondala, T., Scanlan, C., Huflejt, M.E., Alvarez, R., Bryan, M.C., Fazio, F., Calarese, D., Stevens, J., et al. (2004). Printed covalent glycan array for ligand profiling of diverse glycan binding proteins. Proc. Natl. Acad. Sci. USA *101*, 17033–17038.

Chandrasekaran, A., Srinivasan, A., Raman, R., Viswanathan, K., Raguram, S., Tumpey, T.M., Sasisekharan, V., and Sasisekharan, R. (2008). Glycan topology determines human adaptation of avian H5N1 virus hemagglutinin. Nat. Biotechnol. *26*, 107–113.

Childs, R.A., Palma, A.S., Wharton, S., Matrosovich, T., Liu, Y., Chai, W., Campanero-Rhodes, M.A., Zhang, Y., Eickmann, M., Kiso, M., et al. (2009). Receptor-binding specificity of pandemic influenza A (H1N1) 2009 virus determined by carbohydrate microarray. Nat. Biotechnol. *27*, 797–799.

Chu, V.C., and Whittaker, G.R. (2004). Influenza virus entry and infection require host cell N-linked glycoprotein. Proc. Natl. Acad. Sci. USA *101*, 18153–18158.

Connor, R.J., Kawaoka, Y., Webster, R.G., and Paulson, J.C. (1994). Receptor specificity in human, avian, and equine H2 and H3 influenza virus isolates. Virology *205*, 17–23.

de Graaf, M., and Fouchier, R.A. (2014). Role of receptor binding specificity in influenza A virus transmission and pathogenesis. EMBO J. *33*, 823–841.

de Vries, E., de Vries, R.P., Wienholts, M.J., Floris, C.E., Jacobs, M.S., van den Heuvel, A., Rottier, P.J., and de Haan, C.A. (2012). Influenza A virus entry into cells lacking sialylated N-glycans. Proc. Natl. Acad. Sci. USA *109*, 7457–7462.

de Vries, R.P., de Vries, E., Martínez-Romero, C., McBride, R., van Kuppeveld, F.J., Rottier, P.J., García-Sastre, A., Paulson, J.C., and de Haan, C.A. (2013). Evolution of the hemagglutinin protein of the new pandemic H1N1 influenza virus: maintaining optimal receptor binding by compensatory substitutions. J. Virol. *87*, 13868–13877.

Grant, O.C., Tessier, M.B., Meche, L., Mahal, L.K., Foley, B.L., and Woods, R.J. (2016). Combining 3D structure with glycan array data provides insight into the origin of glycan specificity. Glycobiology *26*, 772–783.

Gulati, S., Smith, D.F., Cummings, R.D., Couch, R.B., Griesemer, S.B., St George, K., Webster, R.G., and Air, G.M. (2013). Human H3N2 influenza viruses isolated from 1968 to 2012 show varying preference for receptor substructures with no apparent consequences for disease or spread. PLoS ONE *8*, e66325.

Hardy, C.T., Young, S.A., Webster, R.G., Naeve, C.W., and Owens, R.J. (1995). Egg fluids and cells of the chorioallantoic membrane of embryonated chicken eggs can select different variants of influenza A (H3N2) viruses. Virology *211*, 302–306.

Hatakeyama, S., Sakai-Tagawa, Y., Kiso, M., Goto, H., Kawakami, C., Mitamura, K., Sugaya, N., Suzuki, Y., and Kawaoka, Y. (2005). Enhanced expression of an α2,6-linked sialic acid on MDCK cells improves isolation of human influenza viruses and evaluation of their sensitivity to a neuraminidase inhibitor. J. Clin. Microbiol. *43*, 4139–4146.

Ihara, H., Ikeda, Y., and Taniguchi, N. (2006). Reaction mechanism and substrate specificity for nucleotide sugar of mammalian α1,6-fucosyltransferase–a large-scale preparation and characterization of recombinant human FUT8. Glycobiology *16*, 333–342.

Imai, M., and Kawaoka, Y. (2012). The role of receptor binding specificity in interspecies transmission of influenza viruses. Curr. Opin. Virol. *2*, 160–167.

Jia, N., Barclay, W.S., Roberts, K., Yen, H.L., Chan, R.W., Lam, A.K., Air, G., Peiris, J.S., Dell, A., Nicholls, J.M., and Haslam, S.M. (2014). Glycomic characterization of respiratory tract tissues of ferrets: implications for its use in influenza virus infection studies. J. Biol. Chem. *289*, 28489–28504.

Lakdawala, S.S., Jayaraman, A., Halpin, R.A., Lamirande, E.W., Shih, A.R., Stockwell, T.B., Lin, X., Simenauer, A., Hanson, C.T., Vogel, L., et al. (2015). The soft palate is an important site of adaptation for transmissible influenza viruses. Nature *526*, 122–125.

Lee, H.K., Tang, J.W., Kong, D.H., Loh, T.P., Chiang, D.K., Lam, T.T., and Koay, E.S. (2013). Comparison of mutation patterns in full-genome A/H3N2 influenza sequences obtained directly from clinical samples and the same samples after a single MDCK passage. PLoS ONE *8*, e79252.

Lee, P.S., Ohshima, N., Stanfield, R.L., Yu, W., Iba, Y., Okuno, Y., Kurosawa, Y., and Wilson, I.A. (2014). Receptor mimicry by antibody F045-092 facilitates universal binding to the H3 subtype of influenza virus. Nat. Commun. *5*, 3614.

Li, Y., Bostick, D.L., Sullivan, C.B., Myers, J.L., Griesemer, S.B., Stgeorge, K., Plotkin, J.B., and Hensley, S.E. (2013). Single hemagglutinin mutations that

alter both antigenicity and receptor binding avidity influence influenza virus antigenic clustering. J. Virol. *87*, 9904–9910.

Lin, Y.P., Xiong, X., Wharton, S.A., Martin, S.R., Coombs, P.J., Vachieri, S.G., Christodoulou, E., Walker, P.A., Liu, J., Skehel, J.J., et al. (2012). Evolution of the receptor binding properties of the influenza A(H3N2) hemagglutinin. Proc. Natl. Acad. Sci. USA *109*, 21474–21479.

Markwell, M.A., and Paulson, J.C. (1980). Sendai virus utilizes specific sialyloligosaccharides as host cell receptor determinants. Proc. Natl. Acad. Sci. USA *77*, 5693–5697.

Markwell, M.A., Svennerholm, L., and Paulson, J.C. (1981). Specific gangliosides function as host cell receptors for Sendai virus. Proc. Natl. Acad. Sci. USA *78*, 5406–5410.

Matrosovich, M., Tuzikov, A., Bovin, N., Gambaryan, A., Klimov, A., Castrucci, M.R., Donatelli, I., and Kawaoka, Y. (2000). Early alterations of the receptor-binding properties of H1, H2, and H3 avian influenza virus hemagglutinins after their introduction into mammals. J. Virol. *74*, 8502–8512.

McBride, R., Paulson, J.C., and de Vries, R.P. (2016). A miniaturized glycan microarray assay for assessing avidity and specificity of influenza A virus hemagglutinins. J. Vis. Exp. (111).

Medeiros, R., Escriou, N., Naffakh, N., Manuguerra, J.C., and van der Werf, S. (2001). Hemagglutinin residues of recent human A(H3N2) influenza viruses that contribute to the inability to agglutinate chicken erythrocytes. Virology *289*, 74–85.

Nivedha, A.K., Makeneni, S., Foley, B.L., Tessier, M.B., and Woods, R.J. (2014). Importance of ligand conformational energies in carbohydrate docking: Sorting the wheat from the chaff. J. Comput. Chem. *35*, 526–539.

Nobusawa, E., Ishihara, H., Morishita, T., Sato, K., and Nakajima, K. (2000). Change in receptor-binding specificity of recent human influenza A viruses (H3N2): a single amino acid change in hemagglutinin altered its recognition of sialyloligosaccharides. Virology *278*, 587–596.

Nycholat, C.M., McBride, R., Ekiert, D.C., Xu, R., Rangarajan, J., Peng, W., Razi, N., Gilbert, M., Wakarchuk, W., Wilson, I.A., and Paulson, J.C. (2012). Recognition of sialylated poly-N-acetyllactosamine chains on N- and O-linked glycans by human and avian influenza A virus hemagglutinins. Angew. Chem. Int. Ed. Engl. *51*, 4860–4863.

Oh, D.Y., Barr, I.G., Mosse, J.A., and Laurie, K.L. (2008). MDCK-SIAT1 cells show improved isolation rates for recent human influenza viruses compared to conventional MDCK cells. J. Clin. Microbiol. *46*, 2189–2194.

Paulson, J.C., and de Vries, R.P. (2013). H5N1 receptor specificity as a factor in pandemic risk. Virus Res. *178*, 99–113.

Peng, W., Pranskevich, J., Nycholat, C., Gilbert, M., Wakarchuk, W., Paulson, J.C., and Razi, N. (2012). Helicobacter pylori β1,3-N-acetylglucosaminyltransferase for versatile synthesis of type 1 and type 2 poly-LacNAcs on N-linked, O-linked and I-antigen glycans. Glycobiology *22*, 1453–1464.

Raman, R., Tharakaraman, K., Shriver, Z., Jayaraman, A., Sasisekharan, V., and Sasisekharan, R. (2014). Glycan receptor specificity as a useful tool for characterization and surveillance of influenza A virus. Trends Microbiol. *22*, 632–641.

Seko, A., Koketsu, M., Nishizono, M., Enoki, Y., Ibrahim, H.R., Juneja, L.R., Kim, M., and Yamamoto, T. (1997). Occurence of a sialylglycopeptide and free sialylglycans in hen's egg yolk. Biochim. Biophys. Acta *1335*, 23–32.

Shi, Y., Wu, Y., Zhang, W., Qi, J., and Gao, G.F. (2014). Enabling the 'host jump': structural determinants of receptor-binding specificity in influenza A viruses. Nat. Rev. Microbiol. *12*, 822–831.

Skehel, J.J., and Wiley, D.C. (2000). Receptor binding and membrane fusion in virus entry: the influenza hemagglutinin. Annu. Rev. Biochem. *69*, 531–569.

Skehel, J.J., Stevens, D.J., Daniels, R.S., Douglas, A.R., Knossow, M., Wilson, I.A., and Wiley, D.C. (1984). A carbohydrate side chain on hemagglutinins of Hong Kong influenza viruses inhibits recognition by a monoclonal antibody. Proc. Natl. Acad. Sci. USA *81*, 1779–1783.

Stevens, J., Blixt, O., Paulson, J.C., and Wilson, I.A. (2006). Glycan microarray technologies: tools to survey host specificity of influenza viruses. Nat. Rev. Microbiol. *4*, 857–864.

Stevens, J., Chen, L.M., Carney, P.J., Garten, R., Foust, A., Le, J., Pokorny, B.A., Manojkumar, R., Silverman, J., Devis, R., et al. (2010). Receptor specificity of influenza A H3N2 viruses isolated in mammalian cells and embryonated chicken eggs. J. Virol. *84*, 8287–8299.

Vigerust, D.J., Ulett, K.B., Boyd, K.L., Madsen, J., Hawgood, S., and McCullers, J.A. (2007). N-linked glycosylation attenuates H3N2 influenza viruses. J. Virol. *81*, 8593–8600.

Walther, T., Karamanska, R., Chan, R.W., Chan, M.C., Jia, N., Air, G., Hopton, C., Wong, M.P., Dell, A., Malik Peiris, J.S., et al. (2013). Glycomic analysis of human respiratory tract tissues and correlation with influenza virus infection. PLoS Pathog. *9*, e1003223.

Wang, Z., Chinoy, Z.S., Ambre, S.G., Peng, W., McBride, R., de Vries, R.P., Glushka, J., Paulson, J.C., and Boon, G.J. (2013). A general strategy for the chemoenzymatic synthesis of asymmetrically branched N-glycans. Science *341*, 379–383.

Xu, R., McBride, R., Nycholat, C.M., Paulson, J.C., and Wilson, I.A. (2012). Structural characterization of the hemagglutinin receptor specificity from the 2009 H1N1 influenza pandemic. J. Virol. *86*, 982–990.

Yang, H., Carney, P.J., Chang, J.C., Guo, Z., Villanueva, J.M., and Stevens, J. (2015). Structure and receptor binding preferences of recombinant human A(H3N2) virus hemagglutinins. Virology *477*, 18–31.

Yoon, S.W., Webby, R.J., and Webster, R.G. (2014). Evolution and ecology of influenza A viruses. Curr. Top. Microbiol. Immunol. *385*, 359–375.

Zhang, H., de Vries, R.P., Tzarum, N., Zhu, X., Yu, W., McBride, R., Paulson, J.C., and Wilson, I.A. (2015). A human-infecting H10N8 influenza virus retains a strong preference for avian-type receptors. Cell Host Microbe *17*, 377–384.